



UNIVERSITY OF LEEDS

This is a repository copy of *Temporal analysis of skeletal muscle remodelling post hindlimb ischemia reveals intricate autophagy regulation*.

White Rose Research Online URL for this paper:

<https://eprints.whiterose.ac.uk/192557/>

Version: Accepted Version

Article:

Scalabrin, M orcid.org/0000-0001-6663-7088, Engman, V, Maccannell, A et al. (4 more authors) (2022) Temporal analysis of skeletal muscle remodelling post hindlimb ischemia reveals intricate autophagy regulation. *American Journal of Physiology: Cell Physiology*, 323 (6). C1601-C1610. ISSN 0363-6143

<https://doi.org/10.1152/ajpcell.00174.2022>

© 2022, American Journal of Physiology-Cell Physiology. This is an author produced version of a article published in *American Journal of Physiology-Cell Physiology*. Uploaded in accordance with the publisher's self-archiving policy.

Reuse

Items deposited in White Rose Research Online are protected by copyright, with all rights reserved unless indicated otherwise. They may be downloaded and/or printed for private study, or other acts as permitted by national copyright laws. The publisher or other rights holders may allow further reproduction and re-use of the full text version. This is indicated by the licence information on the White Rose Research Online record for the item.

Takedown

If you consider content in White Rose Research Online to be in breach of UK law, please notify us by emailing eprints@whiterose.ac.uk including the URL of the record and the reason for the withdrawal request.



eprints@whiterose.ac.uk
<https://eprints.whiterose.ac.uk/>

1
2
3
4
5
6
7
8
9
10
11
12
13
14
15
16
17
18
19
20
21
22
23
24
25
26
27
28
29
30
31
32
33

Temporal analysis of skeletal muscle remodelling post hindlimb ischemia reveals intricate autophagy regulation

Mattia Scalabrin¹, Viktor Engman¹, Amanda Maccannell², Annabel Critchlow¹, Lee D. Roberts², Nadira Yudalsheva², T. Scott Bowen¹

1. School of Biomedical Science, Faculty of Biological Science, University of Leeds, UK.

2. Leeds Institute of Cardiovascular and Metabolic Medicine, University of Leeds, UK

Short title: skeletal muscle remodelling following ischemia

Supplementary materials are available at:

DOI: <https://doi.org/10.6084/m9.figshare.20472237>

Corresponding author:

T. Scott Bowen, PhD

School of Biomedical Sciences,

Faculty of Biological Sciences,

University of Leeds, Leeds,

United Kingdom,

LS2 9JT

Tel: (+44) 113 343 3834

Email: t.s.bowen@leeds.ac.uk

34

35 **Abstract**

36 Hind Limb Ischemia (HLI) is the most severe form of peripheral arterial disease,
37 associated with a substantial reduction of limb blood flow that impairs skeletal
38 muscle homeostasis to promote functional disability. The molecular regulators of
39 HLI-induced muscle perturbations remain poorly defined. This study investigated
40 whether changes in the molecular catabolic-autophagy signalling network were
41 linked to temporal remodelling of skeletal muscle in HLI.

42

43 HLI was induced via hindlimb ischemia (femoral artery ligation) and confirmed by
44 Doppler echocardiography. Experiments were terminated at time points defined as
45 early- (7 days; n=5) or late (28 days; n=5) stage HLI. Ischemic and non-ischemic
46 (contralateral) limb muscles were compared. Ischemic vs. non-ischemic muscles
47 demonstrated overt remodelling at early-HLI but normalised at late-HLI. Early-onset
48 fibre atrophy was associated with excessive autophagy signalling in ischemic
49 muscle: protein expression increased for Beclin-1, LC3 and p62 ($p<0.05$) but
50 proteasome-dependent markers were reduced ($p<0.05$). Mitophagy signalling
51 increased in early-stage HLI which aligned with an early and sustained loss of
52 mitochondrial content ($p<0.05$). Upstream autophagy regulators Sestrins showed
53 divergent responses during early-stage HLI (Sestrin2 increased while Sestrin1
54 decreased; $p<0.05$) in parallel to increased AMPK phosphorylation ($p<0.05$) and
55 lower antioxidant enzyme expression. No changes were found in markers for
56 mTORC1 signalling.

57

58 These data indicate early-activation of the sestrin-AMPK signalling axis may regulate
59 autophagy to stimulate rapid and overt muscle atrophy in HLI, which is normalised
60 within weeks and accompanied by recovery of muscle mass. A complex interplay
61 between Sestrins to regulate autophagy signalling during early-to-late muscle
62 remodelling in HLI is likely.

63

64 **Key words:** Ischemia, Skeletal Muscle, Autophagy, Sestrins

65

66 **Abbreviations**

67	4EBP1	Eukaryotic translation initiation factor 4E-binding protein 1
68	AMPK	AMP-activated protein kinase
69	CSA	Cross Sectional Area
70	CuZnSOD	Superoxide Dismutase 1
71	Drp1	Dynamin-like Protein 1
72	GC	Gastrocnemius
73	HLI	Hind Limb Ischemia
74	HO-1	Heme-oxygenase 1
75	LC3	Microtubule-associated Protein 1A/1B-Light Chain 3
76	Mfn2	Mitofusin 2
77	MnSOD	Superoxide Dismutase 2
78	mTORC1	Mechanistic target of rapamycin complex 1
79	MuRF1	Muscle RING-Finger protein-1
80	Nrf-2	Nuclear factor-erythroid factor 2-related factor 2
81	OPA1	Optic Atrophy 1 protein
82	rbS6	Ribosomal protein S6
83	UPS	Ubiquitin Proteasome System

84 **Introduction**

85 Hind Limb Ischemia (HLI) is the most severe form of peripheral vascular disease in
86 humans, affecting over 200 million people worldwide (1-3). HLI reduces lower limb
87 blood flow to cause symptoms of pain and disability, with limb amputation and death
88 also reported (2, 3). A major outcome in HLI patients is severely reduced functional
89 mobility, which worsens within 6 months of diagnosis (4, 5). The underlying
90 mechanisms that contribute towards functional decline in HLI patients are poorly
91 established. Impairments to skeletal muscle homeostasis are strongly implicated,
92 which may include changes related to loss of innervation (6), fibre atrophy,
93 contractile dysfunction, increased ectopic fat deposition and mitochondrial
94 derangements (4). However, there remains a paucity of data explaining what
95 molecular events contribute towards this temporal and functional decline in muscle
96 subjected to HLI.

97

98 HLI is associated with early-onset muscle wasting, which is closely linked with
99 functional disability (7). Muscle mass is controlled by a complex interplay between
100 anabolic and catabolic signalling pathways (8), with macro-autophagy (herein
101 referred to as autophagy) a major catabolic component (9). Autophagy is vital for
102 maintaining cellular homeostasis (10) given its role in delivering dysfunctional
103 proteins and organelles to the autolysosome for degradation (11). However,
104 perturbed regulation leading to sustained increases or decreases in autophagy
105 results in overt muscle pathology (9). Previous studies using different models of HLI
106 including cerebral ischemia (12), ischemia/reperfusion (13) and femoral occlusion
107 (14-16) implicate autophagy as a central mechanism in the muscle wasting process.
108 Noteworthy, autophagy seems to be upregulated early (i.e. within 2 hours post-
109 ischemic injury (15)) but evidence indicates that despite driving atrophy, this
110 activation may promote muscle survival and revascularization (16). Hence,
111 autophagy could be critical for normal muscle regeneration and physiological
112 recovery in HLI.

113

114 Autophagy is regulated by a network complicated mirage of upstream signalling
115 mechanisms (17). Among these, a family of newly discovered small stress-induced
116 proteins called Sestrins have been suggested as potential master regulators of
117 skeletal muscle homeostasis and autophagy (18). The Sestrin family contains three

118 proteins (Sestrin 1-3) (19), with Sestrin 1 and Sestrin 2 being the two isoforms mainly
119 expressed in skeletal muscle (20). Recent evidence further suggest that Sestrins,
120 whose levels decrease in several muscle atrophy conditions and ageing, play a
121 central role as mediators of the beneficial effects of exercise training by protecting
122 skeletal muscle homeostasis (i.e. by regulating autophagy through AMP-activated
123 protein kinase (AMPK) (13, 20)) but also by regulating regeneration via effects on
124 muscle stem cells (21). In addition, Sestrins either directly (via their oxidoreductase
125 activity) or indirectly (via activation of the Nuclear factor-erythroid factor 2-related
126 factor 2 (Nrf2) signalling pathway) modulate oxidative stress in muscle and
127 accumulation of oxidative damage (22).

128

129 Overall whether progressive muscle remodelling following HLI is linked to temporal
130 changes in autophagy signalling is poorly defined (23-26). This study explored the
131 autophagy signalling axis during skeletal muscle remodelling in severe ischemia.
132 Targeting autophagy regulation may offer novel therapeutic targets for patients with
133 HLI.

134

135

136

137

138

139

140 **Materials and Methods**

141 **Animal procedures**

142 Twelve weeks old C57BL/6 male mice (n=10) were included in this study and
143 provided ad libitum access to standard chow and water. Experiments were
144 performed under UK Home Office animal guidelines (Scientific Procedures) Act 1986
145 and received ethical approval from the University of Leeds Animal Welfare Ethical
146 Review Body. The number of mice per group (n=5) was based upon past studies
147 (16, 23, 24, 27) which showed they were powered to detect differences in our
148 primary measure of muscle mass. Mice underwent unilateral surgery to induce HLI in
149 the left lower hindlimb, with the right limb serving as control (i.e. non ischemia). Prior
150 to surgery, mice were anesthetized with a mix of Isoflurane 0.2% and O₂ and
151 alongside received an injection of buprenorphine (analgesic; 1mg/kg sc). The
152 femoral artery and vein were isolated, ligated and then fully dissected to induce
153 ischemia while preventing collateralization, as previously detailed (24, 28, 29). After
154 surgery, the external wound was sutured and mice were maintained in warmed
155 cages until recovery. Mice were sacrificed via cervical dislocation at 7 days (n=5)
156 and 28 days (n=5) and dissected skeletal muscles were weighed then immediately
157 snap frozen in liquid nitrogen and stored at -80°C until further analysis, whereas the
158 soleus was prepared for histological analysis as below.

159

160 **Laser Doppler Flowmetry**

161 Laser Doppler Flowmetry was performed on Moor LDI2-HR (Moor Systems, UK)
162 before, 7 days and 28 days after surgery (23). Briefly, mice were anesthetized with a
163 mix of isoflurane 0.2%, placed on a heated map and kept under anaesthesia
164 throughout the entire duration of the recording. Images were collected and analysed
165 using a MoorLDI software, Version 5.3 (Moor Systems, UK) by comparing the
166 ischemic to non-ischemic limb perfusion ratio, based upon flux below the level of the
167 inguinal ligament.

168

169 **SDS-PAGE western blot**

170 The gastrocnemius (GC) muscles from the left and right limbs were ground in liquid
171 nitrogen and the resulting powder added to 200µl of RIPA buffer (Merk, Darmstadt,
172 Germany) with the addition of Pierce™ Protease and Phosphatase Inhibitor Mini

173 Tablets, EDTA Free (Thermo Fisher Scientific, Waltham, MA, USA). SDS-PAGE and
174 immunoblotting analysis were performed as previously described (30). Ponceau red
175 (Sigma-Aldrich Ltd, Gillingham, Dorset, United Kingdom) was used to verify the
176 effectiveness of transfer procedure and GAPDH (Cell Signalling Technology,
177 Danvers, MA, USA) used as a housekeeping protein to normalize the results.
178 Primary antibodies were detected using recommended HRP-linked secondary
179 antibodies (Cell Signalling Technology, Danvers, MA, USA; see supplementary
180 material Table 1) and Chemiluminescent signal was detected using the G.Box
181 imaging system (Syngene, Cambridge, UK) following addition of ECL (Thermo
182 Fisher Scientific, Waltham, MA, USA). Analysis of densitometry was performed using
183 ImageJ software, as previously described (30). A representative image of the protein
184 ladder (Thermo Fisher Scientific, Waltham, MA, USA) used to determine the
185 molecular weights during the experiments is presented in Supplementary Figure 1.

186

187 **Immunohistochemical analysis**

188 Soleus muscles were mounted directly on a cork disk, surrounded with O.C.T.
189 mounting medium (Thermo Fisher Scientific, Waltham, MA, USA), frozen rapidly in
190 isopentane cooled in liquid nitrogen and sectioned (12 μ m) using a cryostat (Leica
191 CM1850, Leica, Wetzlar, Germany) as previously described (31). To assess fibre
192 cross-sectional area (CSA) and fibre type distribution, sections were re-hydrated and
193 blocked for 1 hour in 5% Goat Serum (Thermo Fisher Scientific, Waltham, MA, USA)
194 + M.O.M. Blocking (Vector Lab, Burlingame, CAL, USA). Sections were then
195 incubated for 60 minutes with BA-D5 (IgG2B, 1:250 - MyHCI fibres) and SC-71
196 (IgG1, 1:250 - MyHCIIa fibres) (Developmental Studies Hybridoma Bank, Iowa City,
197 IA, USA) and respective secondary antibodies (conjugated goat anti-mouse IgG2b,
198 1:500 - Thermo Fisher Scientific, Waltham, MA). Muscle fibre boundaries were
199 labelled using Wheat Germ Agglutinin, Rhodamine (1:1000; Vector Lab, Burlingame,
200 CAL, USA). Slides were then imaged at magnifications of x20 using the Zeiss
201 Axioscan Z1 slides scanner (Zeiss AG, Jena, Germany). Sections were analysed
202 using Myovision (University of Kentucky) and ImageJ software. To stain for fibres
203 boundaries and nuclei localisation, sections were fixed with 100% ice-cold methanol
204 and then incubated for 10 minutes in Wheat Germ Agglutinin, Rhodamine (1:1000;
205 Vector Lab, Burlingame, CAL, USA). Slides were then mounted using a mounting

206 media with DAPI (Vector Lab, Burlingame, CAL, USA) and visualised on a Zeiss
207 Axioscan Z1 slides scanner (Zeiss AG, Jena, Germany).

208

209 **Citrate synthase assay**

210 The citrate synthase assay was performed using a previously published protocol
211 (32). Briefly, GC muscles were cryopulverised and resulting powder added to 200µl
212 of RIPA buffer (Merk, Darmstadt, Germany) with the addition of Pierce™ Protease
213 and Phosphatase Inhibitor Mini Tablets, EDTA Free (Thermo Fisher Scientific,
214 Waltham, MA, USA). Samples were sonicated 3 times for 15 sec and centrifuged at
215 12,000g for 10 min at 4°C. Supernatant was collected and protein content quantified
216 using the BCA assay. Citrate synthase activity was measured by detecting the
217 transfer of sulfhydryl groups to 5,5'-dithiobis (2-nitrobenzoic acid) (DTNB) at a
218 wavelength of 412nm with readings performed every 20 seconds for a total of 6
219 minutes using a PowerWave HT plate reader (BioTek, Vermont, Canada). Before
220 performing the assay, 1µl of sample were added to the plate reader together with
221 199µl of the reaction solution (100 mM Tris · HCl, 0.2 mM acetyl CoA, 0.1 mM
222 DTNB; pH 8.1) and incubated for 5 minutes at 37°C. Following incubation, an
223 endpoint reading of the background signal was performed before adding 10µl of
224 Oxaloacetate (10mM) to begin the experiment. Each sample was run in triplicate,
225 means normalised to protein content and calculated as µmol/min/mg; data are
226 presented as percentage of control.

227

228 **Statistical Analysis**

229 Statistical analysis was performed using IBM SPSS statistic version 22 software
230 (IBM analytics, New York, USA). All tests were carried out with a 95% confidence
231 interval and the level of significance was set at 0.05. Normal distribution was
232 checked using the Shapiro-Wilk test while the Levene's test was used to verify the
233 Equality of Variance in our groups. Data was expressed as the mean ± standard
234 error mean (SEM). Independent sample two-tailed t-test was used to detect
235 differences between the control and the ischemic groups, unless otherwise noted.
236 When the normality of distribution assumption was not met, the Mann-Whitney U test
237 was used. Outliers were detected using the established ROUT statistical method
238 (33) and the recommended Q (maximum desired False Discovery Rate) of 1%, with
239 the final sample size for each experiment noted in each figure legend.

241 **Results**

242 **Limb blood flow and muscle remodelling post ischemia**

243 HLI was confirmed by analysing pre- and post-limb perfusion in the control vs.
244 ligated limb (Figure 1a). At 7 days post-surgery, the mean blood flux in the lower
245 hind limb was impaired vs. contralateral limb by (-73%; $U(8) = -2.611$, $p < 0.05$; Figure
246 1b). However, perfusion was increased at 28 days post-surgery by one third (-44%;
247 $p > 0.05$; Figure 1c) indicative of partial revascularization of the lower hindlimb.
248 Despite limited total body mass change (Fig. 1d, e), 7 days of HLI resulted in loss of
249 muscle wet-mass vs. contralateral limb (both GC and soleus; $p < 0.05$; Figure 1f, h).
250 Histological evidence reinforced this finding, with soleus fibre cross-sectional area
251 showing atrophy at 7 days ($t(8) = 2.51$, $p < 0.05$; Figure 2a-b) alongside altered fibre
252 composition (i.e. shift from type I to type IIa $p < 0.05$; Figure 2c). In contrast, at 28
253 days post HLI wet-mass in GC muscle increased vs control ($t(5.6) = -3.243$, $p < 0.05$;
254 Figure 1g), despite no differences in soleus wet-mass, fibre cross-sectional area or
255 composition ($p > 0.05$; Figure 2d-f). Interestingly, soleus showed reappearance of type
256 I fibres towards control levels and a robust regenerative potential at 28 days, as
257 demonstrated by increased fibres with centralised nuclei (+68%) in ischemic muscle
258 that was in general absent in contralateral ($t(8) = -5.731$; $p < 0.05$; Figure 2g-h).

259

260 **Catabolic signalling via autophagy is activated at early HLI stages**

261 Given the finding of early-onset muscle wasting after 7 days HLI, we first explored
262 key catabolic signalling pathways. To monitor the progression of autophagy
263 signalling following ischemia-induced fibre atrophy, several markers were
264 investigated in the GC muscle. Beclin-1 protein content, a reliable marker of
265 autophagy initiation (34), was increased by 6 fold vs. contralateral muscle
266 ($t(8) = 4.943$, $p < 0.05$; Figure 3a) but normalised to control levels at 28 days ($p > 0.05$;
267 Figure 3b). A similar trend was found with microtubule-associated protein 1A/1B-light
268 chain 3 (LC3), a reliable marker of autophagosome formation (34), with increased
269 protein content of both LC3-I ($t(8) = 14.133$, $p < 0.05$; Figure 3c) and LC3-II ($t(8) = 1.965$,
270 $p < 0.05$; Figure 3e) after 7 days in ischemic vs. contralateral muscle with a similar
271 trend seen in the ratio of these two proteins which did not reach statistical
272 significance ($p > 0.05$; figure 3 i). However at 28 days, protein content of LC3-I and
273 LC-II and their ratio were normalised in ischemic muscle to contralateral control
274 values ($p > 0.05$; Figure 3d, f, l). Supporting the hypothesis of increased activation of

275 autophagy at early but not late stages of HLI; protein expression of p62 (SQSTM1)
276 was decreased in ischemic vs. control muscle at 7 days ($t(8)=1.632$, $p<0.05$; Figure
277 3g) but normalised at 28 days ($p>0.05$; Figure 3h). In addition to autophagy, a major
278 pathway mediating muscle wasting is the ubiquitin proteasome system (UPS) which
279 is regulated in part by increased expression of key E3 ligases (termed atrogenes, i.e.
280 MuRF1 and MAFbx). In contrast to increased autophagy signalling at 7 days, while
281 MAFbx/Atrogin-1 tended to decrease but without reaching significance ($t(8)=0.28$,
282 $p>0.05$; Supplementary Figure 1a), MuRF1 protein content was decreased in
283 ischemic muscle ($t(8)=3.099$, $p<0.05$; Supplementary Figure 1c). At 28 days,
284 however, atroгене expression was normalised in line with autophagy signalling
285 ($p>0.05$; Supplementary Figure 1d). Overall these data indicate autophagy signalling
286 is activated at early HLI stages but with potential inhibition of proteasome-dependent
287 catabolic activity.

288

289 **Mitophagy and mitochondria**

290 An important aspect of autophagy is mitophagy, which maintains mitochondrial
291 quality control by recycling mitochondrial proteins to preserve metabolic reserve.
292 Mitophagy markers including phosphorylated dynamin-like protein 1 (Drp1; a marker
293 of mitochondrial fission) increased at 7 days HLI ($U(8)= -1.72$, $p<0.05$; Figure 4a)
294 despite no difference between groups for optic atrophy 1 protein (OPA-1- $p>0.05$;
295 Figure 4c) and Mitofusin 2 (Mfn2 - $p>0.05$; Figure 4e) two markers of mitochondria
296 fusion. After 28 days, both Drp1, OPA1 and Mfn2 were not different between
297 conditions ($p>0.05$, Figure 4b, d, f). Given these early changes in mitophagy
298 markers, we next measured citrate synthase activity in order to provide an index of
299 mitochondrial content. Citrate synthase activity was decreased at 7 days HLI
300 ($t(8)=4.568$, $p<0.05$; Figure 4f) and remained reduced at 28 days compared to
301 contralateral muscle ($t(4.4)=3.27$, $p<0.05$; Figure 4g), which indicates an early and
302 sustained loss of muscle mitochondrial content in HLI muscles.

303

304 **Temporal-dependent changes in Sestrins may regulate autophagy in HLI**

305 Given our findings indicated that early muscle loss in HLI is associated with robust
306 autophagy signalling alongside apparent inhibition of proteasome signalling, we next
307 explored upstream regulators of autophagy. We first investigated whether the
308 expression of the Sestrins family, known to influence autophagy-dependent muscle

309 remodelling, was altered in HLI. Protein content of Sestrin 1 tended to decreased by
310 1-fold 7 days following HLI vs. contralateral control muscle ($t(4.2)=3.832$, $p<0.05$;
311 Figure 5a). This was in contrast to Sestrin 2, where protein expression increased by
312 2-fold ($t(4.3)=-4.281$, $p<0.05$. Figure 5c). After 28 days HLI, both Sestrin 1 and
313 Sestrin 2 expression were normalised to control values ($p>0.05$; Figure 5b, d).
314 Together, these findings suggest that a complex interplay exists between Sestrin 1
315 and 2 expression that could impact autophagy signalling during muscle remodelling
316 in HLI. As Sestrins regulate autophagy (and UPS) by modulating AMP-activated
317 protein kinase (AMPK) which phosphorylation increased in HLI at 7 days ($t(5)=-$
318 3.755 , $p<0.05$; Figure 5e) but normalised to control levels in HLI 28 days ($p>0.05$;
319 Figure 6f).

320

321 Sestrins have inherent antioxidant properties and also regulate redox homeostasis
322 via Nrf2. As muscle biopsies from HLI patients show oxidative damage (4), we next
323 assessed antioxidant expression profile. At 7 days post HLI, expression of the mainly
324 cytosolic antioxidant superoxide dismutase 1 (CuZnSOD) was decreased
325 ($t(8)=3.827$, $p<0.05$; Figure 5g) while the mitochondrial isoform belonging to the
326 same family, superoxide dismutase 2 (MnSOD) tended to be reduced but without
327 reaching significance ($t(5.09)=1.569$, $p=0.177$; Figure 5i). However, at 28 days
328 antioxidant expression was normalised to control and no differences observed in
329 CuZnSOD or MnSOD following HLI ($p>0.05$; Figure 5h, l). Furthermore, we did not
330 detect differences in the content of Heme Oxygenase 1 at both 7 and 28 days (HO-1
331 - $p>0.05$, Supplementary figure 1e, f), a Nrf2 regulated enzyme that offers oxidative
332 and inflammatory protection. Overall, these data suggest HLI perturbs Sestrin
333 signalling in line with autophagy activation and an overall downregulated antioxidant
334 expression.

335

336 **Markers for anabolic signalling were unchanged in HLI**

337 Given the recovery of muscle mass and cross-sectional area seen in the late-HLI
338 group, we investigated whether HLI was affecting regulation of protein synthesis in
339 skeletal muscle by measuring two key readouts in the mTORC1 signalling pathway.
340 Phosphorylation levels eukaryotic translation initiation factor 4E-binding protein 1
341 (4EBP1) and ribosomal protein S6 (rbS6) remained unchanged in ischemic vs.
342 contralateral muscle both at 7 and 28 days ($p>0.05$; Figure 6a-d).

343

344

345

346 **Discussion**

347 Our understanding of the mechanisms that cause muscle-related disability in
348 patients with HLI remains partially resolved. In the present study, by investigating a
349 temporal experimental model of HLI, we showed that muscle wasting occurred at
350 early-stage (7 days) but was fully normalised within weeks at late-stage (28 days).
351 Early-onset muscle wasting was closely mirrored by a robust increase in markers of
352 catabolic-autophagy signalling. Early and sustained loss of mitochondria content in
353 HLI was closely associated with dysregulated expression of mitophagy proteins. Our
354 data indicate HLI may modulate the sestrin-autophagy signalling axis to drive loss of
355 muscle mass, given sestrin 2 was upregulated early in parallel to reduced antioxidant
356 enzyme expression. Surprisingly, a divergent pattern for sestrin 1 expression was
357 found, which raises the question of whether cross-talk or redundancy exists in
358 sestriins following HLI to impact muscle mass.

359

360 *Muscle atrophy is associated with activated autophagy in HLI*

361 Patients with HLI experience changes to muscle homeostasis that cause severe
362 muscle wasting and disability (1, 4, 7, 23, 35, 36). A lack of consensus on the
363 mechanisms responsible exist however, in particular regarding the role of autophagy.
364 In the present study, 7 days following HLI we reported a decreased blood flow
365 compared to the control limb (>70%) which translated to reductions in muscle mass
366 (both GC and soleus). This muscle wasting is attributed to a 20% reduction in overall
367 fibre CSA and an absolute loss of Type I fibres following HLI, with recent
368 suggestions that hypoxia (both environmental and pathological) may underlie such
369 changes (37). Several different pathways are known to drive skeletal muscle atrophy
370 and in particular the UPS and autophagy (38). The UPS is upregulated in several
371 conditions characterised by muscle wasting (38) with MuRF1 and Atrogin-1 shown to
372 play a pivotal role in this pathway. Our analysis showed that in ischemic muscle
373 MuRF1 and Atrogin-1 expression is decreased when compared to the contralateral
374 leg suggesting that during ischemia the muscle wasting in HLI may not be driven
375 exclusively by the UPS but rather by alternative pathways. However, it is worth
376 mentioning that a previous study (39) reported hyperactivation of these enzymes at
377 early stages post-HLI suggesting that, while the UPS may play an important role in
378 the immediate aftermath of the ischemic injury, in the long-term its role may become
379 secondary.

380 Several different pathways drive muscle atrophy, including autophagy (8). Autophagy
381 is an important pathway allowing maintenance of cellular homeostasis but when
382 dysregulated triggers muscle wasting (40, 41). Our data suggest that HLI causes
383 early increases in muscle Beclin-1, LC3-I and LC3-II protein content. These proteins
384 play an important role in regulating autophagosome induction and maturation and
385 are considered reliable markers of autophagy (42). We also found a decrease in the
386 protein expression of p62, a cargo protein responsible for delivering dysfunctional
387 proteins and organelles to the autolysosome for degradation being degraded itself in
388 the process (10). Cellular content of p62 protein content is inversely correlated to
389 autophagy (43), therefore low p62 expression reinforces our hypothesis that
390 autophagy is upregulated in HLI and serves as a key trigger for early-onset muscle
391 wasting. Autophagy acts to maintain a healthy pool of mitochondria in a process
392 known as mitophagy which can become unbalanced, thus eliminating damaged and
393 dysfunctional mitochondria and forgoing quantity over quality (11). This is particularly
394 relevant in HLI where muscle biopsies from patients have reduced mitochondrial
395 number (4). At 7 days post HLI, our data confirmed loss of mitochondria content in
396 line with disturbed mitophagy (i.e. increased fission), as evidenced by elevated Drp1
397 phosphorylation (44) despite no change to markers of fusion. Mitochondria loss was
398 sustained at 28 days following HLI, despite mitophagy markers and muscle size
399 recovering. A disconnection between muscle mass/function and mitochondria activity
400 does not seem to be uncommon in HLI, with a recent patient study showing that, in
401 response to exercise, improved muscle function and fibre CSA were not associated
402 with changes in mitochondria number and activity [45]. The meaning behind the lack
403 of recovery in mitochondrial properties compared to muscle mass remains
404 unexplored in ischemic conditions and further studies are warranted. For example,
405 this lag in recovery of muscle mitochondria compared to mass may explain
406 prolonged fatigue-related symptoms experienced by HLI patients.

407

408 *Molecular regulators of autophagy in HLI via AMPK and Sestrins*

409 Several proteins are involved in maintaining a tight balance between cellular
410 anabolism and catabolism, and specifically autophagy regulation. Among these,
411 mTORC1 plays a pivotal role in orchestrating anabolic and catabolic responses to
412 environmental changes including autophagy inhibition (45) (46). No changes in
413 reliable mTORC1 downstream signalling markers (4EBP1 and rS6) were found post

414 HLI and, despite being unable to exclude that the mTORC1 axis remains unaffected
415 during HLI, further studies are warranted to determine levels of mTORC1 activation
416 in HLI. To further investigate other molecular regulators of autophagy, we found
417 phosphorylation levels of AMPK were increased following HLI at 7 days. Once
418 phosphorylated, AMPK, a central energy sensor regulating cellular metabolism and
419 energy homeostasis, promotes autophagy and mitophagy via several pathways.
420 Specifically, it is known that AMPK can promote autophagy directly through the
421 phosphorylation of specific targets in the mTORC1, ULK1 and PIK3C3/VPS34
422 complexes but also by regulating transcription factors such as FOXO3, Transcription
423 factor EB and Bromodomain-containing protein 4 (47). Overall, our data suggest that
424 upon induction of HLI, AMPK-dependent autophagy activation likely serves to
425 accelerate muscle remodelling that exacerbate early muscle loss. Further studies are
426 warranted to determine the specific pathway of AMPK-autophagy activation in early
427 HLI.

428

429 Sestrins are regarded to be critical for maintenance of skeletal muscle homeostasis
430 (20). Sestrins control autophagy to promote proteostasis that preserves muscle
431 mass and function (18). We found Sestrin 1 content decreased but Sestrin 2
432 increased early following HLI. Is reduced Sestrin 1 content a compensatory response
433 to elevated Sestrin 2 levels? Past studies have shown that in sarcopenic muscle,
434 Sestrin 1 expression tends to decrease similar to our data in HLI (20). In contrast to
435 Sestrin 1, Sestrin 2 is activated under hypoxic conditions induced by ischemic injury
436 as most widely characterised in myocardial ischemia/reperfusion injury (48). Lower
437 oxygen perfusion to ischemic muscle (15, 49, 50) may promote Sestrin 2 activation
438 (28). Sestrin 2 regulates skeletal muscle homeostasis (48), which includes playing a
439 pivotal role in autophagy regulation via AMPK signalling (51). It has been previously
440 reported that Sestrin 2 can induce AMPK phosphorylation via the Serine/threonine
441 kinase 11 to promote autophagy activation (48). By phosphorylating AMPK, Sestrin 2
442 appears to be a central regulator of the autophagic response following HLI. While
443 this may initially contribute to the wasting process, it may also be essential for
444 supporting long-term muscle mass survival and regeneration (16, 52). For example,
445 administration to ischemic mice of the autophagy inhibitor chloroquine reduced
446 muscle function and regenerating potential of myocytes, despite initially conferring
447 protection against muscle wasting (16, 52). Our data support this hypothesis, as 28

448 days following HLI we found a recovery of muscle mass that was associated with
449 normalised fibre CSA, reappearance of type I fibres, and appearance of centralised
450 nuclei (i.e. a marker of fibre regeneration that is commonly observed during skeletal
451 muscle repair following injury (53, 54)). The progressive improvement of the skeletal
452 muscle morphology, together with the metabolic changes reported, suggest that
453 despite the initial response to HLI causing early-onset muscle wasting, this may be
454 an important physiological response regulated by Sestrin 2 and AMPK that overall
455 aims to protect muscle survival and enhance recovery under the most extreme
456 stresses.

457

458 Another important role Sestrins may play in skeletal muscle is as antioxidants (i.e
459 directly or via regulating the NRF2 antioxidant signalling pathway) (20). While the
460 intrinsic catalytic activity of Sestrin 2 as an antioxidant remains unclear (48), there is
461 evidence to suggest it promotes transcription of specific antioxidant genes including
462 superoxide dismutase and Heme-oxygenase 1 (48). Due to limited tissue availability,
463 we were only able to measure the protein content of some antioxidant enzymes and
464 future studies aimed to further explore the interaction between sestrins and the
465 NRF2 antioxidant system in HLI are warranted. Our data showed that the protein
466 content of the antioxidant enzymes CuZnSOD and MnSOD were decreased in HLI
467 compared to control while HO-1 remain unchanged (Supplementary figure 1), which
468 aligns with other atrophic conditions characterised by oxidative stress (43, 48) and
469 that was reported by a previous study in HLI C57Bl/6 female mice (55).

470

471 **Conclusions**

472 In conclusion, we have shown that HLI triggers robust remodelling in skeletal muscle
473 structure including early-onset muscle atrophy loss at 7 days that is normalised later
474 at 28 days. Early muscle wasting following HLI muscles was associated with
475 activated catabolic-autophagy signalling, which was closely linked to Sestrin2-AMPK
476 signalling. Sestrins could act as potential upstream regulators of autophagy-
477 dependent early muscle loss following HLI.

478

479 **Acknowledgments**

480 The authors would also like to thank Natallia Makova and Anna Skromna for their
481 excellent assistance supporting Laser Doppler measurements and Dr Diana Renteria

482 Ramirez for her assistance in samples preparation. This work was supported by
483 MRC UK (MR/S025472/1) and Defence And Security Accelerator (DASA -
484 ACC2011654). The authors declare no conflict of interest.

485

486 **Figures legend**

487

488 **Figure 1.** Representative images of blood flow in the lower hind limbs before (Pre-Op), 7
489 Days and 28 Days after surgery (**a**). At 7 days post-HLI, blood flow (red/yellow) was
490 significantly reduced in ischemic leg (-73%, $p < 0.001$ - **b**) compared to contralateral limb.
491 However, at 28 days post-ischemia, the blood flow was partially restored (-44%, $p > 0.05$ - **c**)
492 as a result of femoral artery collateralization. No differences in total body weight were seen 7
493 days post-HLI ($p > 0.05$ - **d**) while a significant increase was seen in total body weight after
494 surgery at 28 days ($p < 0.05$ - **e**). Muscle wet weight was significantly decreased in the GC
495 ($p < 0.01$ - **f**) and soleus ($p < 0.05$ - **h**) 7 days post-HLI but recovered at 28 days in both GC (**g**)
496 and Soleus (**i**). Histograms represent the mean and the standard error of the mean for each
497 experimental group (n=10). * $p < 0.05$ - ** $p < 0.01$ - *** $p < 0.001$ compared with the control
498 group.

499 **Figure 2.** Representative images of sections from non-ischemic (control) and 7 days post-
500 HLI soleus muscle stained for MyHC isoforms (Type I - red, Type IIa - green, Type IIb/x -
501 black, fibre boundaries - blue) (**a, d**). At 7 days post-HLI there is a significant reduction of
502 fibre CSA (n=8, $p < 0.01$ - **b**) with an absolute loss of type I fibres (n=8, -20%, $p < 0.01$ - **c**)
503 compared to contralateral limb. In line with the recovery of muscle mass seen at 28 days
504 post-HLI, CSA is recovered with no differences compared to the contralateral limb (n=10,
505 $p > 0.05$ - **e**) and with reappearance of type I fibres (n=8, $p > 0.05$ - **f**). A robust regenerative
506 potential at 28 days was confirmed by a significant increase in fibres with centralised nuclei
507 in the ischemic muscle compared to contralateral (n=10, +68 - $p < 0.01$ - **g, h**). Histograms
508 represent the mean and the standard error of the mean for each experimental group. *
509 $p < 0.05$ - ** $p < 0.01$ - *** $p < 0.001$ compared with the control group.

510 **Figure 3.** Several markers of autophagy were investigated in the gastrocnemius muscle.
511 Beclin-1, a reliable marker of autophagy induction was significantly increased in the ischemic
512 muscle 7 days post-HLI ($p < 0.05$ - **a**). Similar trends were seen in both isoforms of LC3, a
513 reliable marker of autophagosome formation ($p < 0.05$ - **c, e**). Protein expression of p62,
514 another reliable marker of autophagy which levels have been inversely correlated to
515 autophagy activity, is instead decreased ($p < 0.01$ - **g**) in ischemic muscle 7 days post-HLI
516 reinforcing our hypothesis that autophagy is up-regulated and is responsible for the loss of
517 muscle mass seen. At 28 days post-HLI, when there is recovery of muscle mass and

518 regeneration, the levels of Beclin-1 (**b**), LC3I (**d**), LC3II (**f**) and p62 (**h**) in the ischemic
519 muscle are no different compared to the levels recorded in the contralateral limb.
520 Representative images of blots were presented (**i**). Histograms represent the mean and the
521 standard error of the mean for each experimental group (n=10). * p<0.05 - ** p<0.01 - ***
522 p<0.001 compared with the control group.

523 **Figure 4.** Unregulated mitophagy was seen at 7 days post HLI with an increase of Drp1
524 phosphorylation (n=9, p<0.01) a marker of mitochondrial fission (**a**) while no changes in
525 OPA1 content were observed (n=10, p>0.05 - **c**). At 28 days post-HLI the levels of Drp1
526 phosphorylation returned to contralateral levels (n=10, p>0.05 - **b**) with no differences seen
527 also in the content of OPA1 (n=10, p>0.05 - **d**). At 7 days post-HLI dysregulated mitophagy
528 resulted in a loss of mitochondria measured using the citrate synthase assay (n=10, p<0.01 -
529 **f**) which was sustained up to 28 days post-HLI (n=10, p<0.05 - **g**) despite the normalisation
530 of mitophagy. No differences were seen in Mfn2 content at 7 (n=8, p>0.05 - **e**), and 28 days
531 (n=10, p>0.05 - **f**). Representative images of blots were presented (**g**). Histograms represent
532 the mean and the standard error of the mean for each experimental group. * p<0.05 - **
533 p<0.01 - *** p<0.001 compared with the control group.

534 **Figure 5.** A different response was seen at 7 days post-HLI in the levels of the two subunits
535 belonging to the Sestrin family analysed in this study. The levels of Sestrin 1 were reduced
536 (n=10, p<0.01 - **a**) while Sestrin 2 were upregulated (n=8, p<0.01 - **c**) suggesting a possible
537 compensatory cross-talk between the two proteins. In line with the increase of Sestrin 2
538 levels, the phosphorylation levels of AMPK were increased (n=8, p<0.01 - **e**). The levels of
539 CuZnSOD were significantly decreased 7 days post-HLI (n=10, p<0.01 - **g**) with a similar
540 trend seen in MnSOD (n=10, p>0.05 - **i**). At 28-days post-HLI, the levels of Sestrin 1 (**b**),
541 Sestrin 2 (**d**), the phosphorylation levels of AMPK (**f**), CuZnSOD (**h**) and MnSOD (**l**)
542 returned to contralateral levels (n=10, p>0.05). Representative images of blots were
543 presented (**m**). Histograms represent the mean and the standard error of the mean for each
544 experimental group. * p<0.05 - ** p<0.01 - *** p<0.001 compared with the control group.

545 **Figure 6.** The downstream readings of the mTORC1 signalling pathway 4EBP1 (**a, c**) and
546 s6rb (**b, d**) were unchanged at 7 and 28 days post-HLI suggesting no activation of this
547 signalling pathway. Representative images of blots were presented (**e**). Histograms
548 represent the mean and the standard error of the mean for each experimental group.

549 **Supplementary Figure 1.** The levels of MuRF1 were decreased 7 days post-HLI (n=10,
550 p<0.05 - **a**) with a similar trend seen for Atrogin-1 (n=9, p>0.05 - **c**) suggesting that the
551 Ubiquitin Proteasome System is not apparently driving muscle remodelling at 7 days after
552 ischemic injury . The levels of MuRF1 returned to contralateral levels 28 days post-HLI
553 (n=10, p>0.05 - **b**) while we were unable to detect readings for Atrogin-1. No differences

554 were detected in the content of HO-1, an antioxidant response element activated by NRF2,
555 both at 7 (n=10, p>0.05 - **e**) and 28 days (n=10, p>0.05 - **f**). Representative images of blots
556 were presented (**g**) together with a representative protein ladder used for our experiments
557 (**h**). Histograms represent the mean and the standard error of the mean for each
558 experimental group. * p<0.05 - ** p<0.01 - *** p<0.001 compared with the control group.

559 **Supplementary table.** List of the antibodies used for SDS-PAGE western blot analysis.

560

561 **References**

562

- 563 1. **Fowkes FGR, Rudan D, Rudan I, Aboyans V, Denenberg JO, McDermott MM, Norman PE,**
564 **Sampson UKA, Williams LJ, Mensah GA, and Criqui MH.** Comparison of global estimates of
565 prevalence and risk factors for peripheral artery disease in 2000 and 2010: a systematic review and
566 analysis. *The Lancet* 382: 1329-1340, 2013.
- 567 2. **Nativel M, Potier L, Alexandre L, Baillet-Blanco L, Ducasse E, Velho G, Marre M, Roussel R,**
568 **Rigalleau V, and Mohammedi K.** Lower extremity arterial disease in patients with diabetes: a
569 contemporary narrative review. *Cardiovasc Diabetol* 17: 138, 2018.
- 570 3. **Weitz JI, Byrne J, Clagett GP, Farkouh ME, Porter JM, Sackett DL, Strandness DE, Jr., and**
571 **Taylor LM.** Diagnosis and treatment of chronic arterial insufficiency of the lower extremities: a
572 critical review. *Circulation* 94: 3026-3049, 1996.
- 573 4. **McDermott MM, Ferrucci L, Gonzalez-Freire M, Kosmac K, Leeuwenburgh C, Peterson CA,**
574 **Saini S, and Sufit R.** Skeletal Muscle Pathology in Peripheral Artery Disease: A Brief Review.
575 *Arterioscler Thromb Vasc Biol* 40: 2577-2585, 2020.
- 576 5. **McDermott MM, Guralnik JM, Criqui MH, Ferrucci L, Liu K, Spring B, Tian L, Domanchuk K,**
577 **Kibbe M, Zhao L, Lloyd Jones D, Liao Y, Gao Y, and Rejeski WJ.** Unsupervised exercise and mobility
578 loss in peripheral artery disease: a randomized controlled trial. *J Am Heart Assoc* 4: 2015.
- 579 6. **Hiatt WR, Regensteiner JG, Wolfel EE, Carry MR, and Brass EP.** Effect of exercise training on
580 skeletal muscle histology and metabolism in peripheral arterial disease. *J Appl Physiol (1985)* 81:
581 780-788, 1996.
- 582 7. **McDermott MM.** Functional impairment in peripheral artery disease and how to improve it
583 in 2013. *Curr Cardiol Rep* 15: 347, 2013.
- 584 8. **Scalabrin M, Adams V, Labeit S, and Bowen TS.** Emerging Strategies Targeting Catabolic
585 Muscle Stress Relief. *Int J Mol Sci* 21: 2020.
- 586 9. **Neel BA, Lin Y, and Pessin JE.** Skeletal muscle autophagy: a new metabolic regulator. *Trends*
587 *Endocrinol Metab* 24: 635-643, 2013.
- 588 10. **Rusten TE, and Stenmark H.** p62, an autophagy hero or culprit? *Nat Cell Biol* 12: 207-209,
589 2010.
- 590 11. **Ji LL, and Yeo D.** Mitochondrial dysregulation and muscle disuse atrophy. *F1000Res* 8: 2019.
- 591 12. **Desgeorges MM, Devillard X, Toutain J, Divoux D, Castells J, Bernaudin M, Touzani O, and**
592 **Freyssenet DG.** Molecular mechanisms of skeletal muscle atrophy in a mouse model of cerebral
593 ischemia. *Stroke* 46: 1673-1680, 2015.
- 594 13. **Liu C, Peng M, Zheng L, Zhao Y, Wang R, Su Q, Chen S, and Li Z.** Enhanced autophagy
595 alleviates injury during hindlimb ischemia/reperfusion in mice. *Exp Ther Med* 18: 1669-1676, 2019.
- 596 14. **Albadawi H, Oklu R, Milner JD, Uong TP, Yoo HJ, Austen WG, Jr., and Watkins MT.** Effect of
597 limb demand ischemia on autophagy and morphology in mice. *J Surg Res* 198: 515-524, 2015.
- 598 15. **Jeong IH, Bae WY, Choi JS, and Jeong JW.** Ischemia induces autophagy of endothelial cells
599 and stimulates angiogenic effects in a hindlimb ischemia mouse model. *Cell Death Dis* 11: 624, 2020.

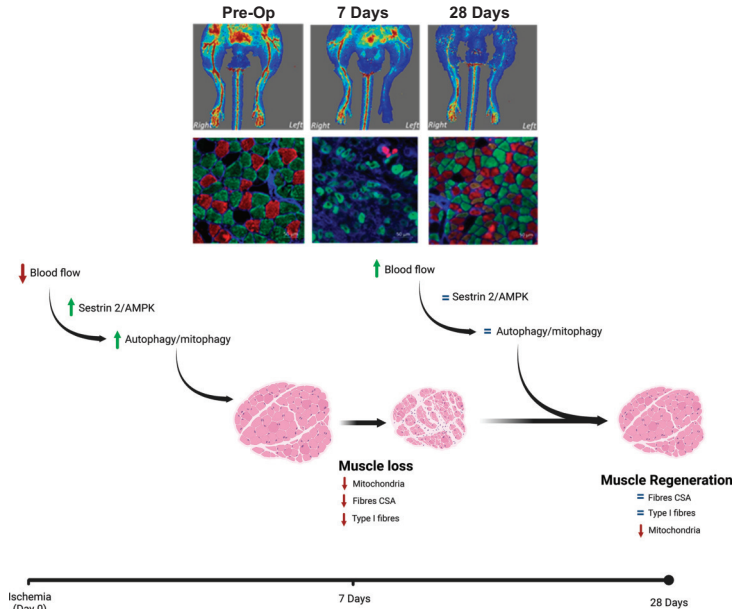
- 600 16. **Sachdev U, Ferrari R, Cui X, Pius A, Sahu A, Reynolds M, Liao H, Sun P, Shinde S, Ambrosio**
601 **F, Shiva S, Loughran P, and Scott M.** Caspase1/11 signaling affects muscle regeneration and
602 recovery following ischemia, and can be modulated by chloroquine. *Mol Med* 26: 69, 2020.
- 603 17. **He C, and Klionsky DJ.** Regulation mechanisms and signaling pathways of autophagy. *Annu*
604 *Rev Genet* 43: 67-93, 2009.
- 605 18. **Segales J, Perdiguero E, Serrano AL, Sousa-Victor P, Ortet L, Jardi M, Budanov AV, Garcia-**
606 **Prat L, Sandri M, Thomson DM, Karin M, Hee Lee J, and Munoz-Canoves P.** Sestrin prevents atrophy
607 of disused and aging muscles by integrating anabolic and catabolic signals. *Nat Commun* 11: 189,
608 2020.
- 609 19. **Pasha M, Eid AH, Eid AA, Gorin Y, and Munusamy S.** Sestrin2 as a Novel Biomarker and
610 Therapeutic Target for Various Diseases. *Oxid Med Cell Longev* 2017: 3296294, 2017.
- 611 20. **Kim M, Sujkowski A, Namkoong S, Gu B, Cobb T, Kim B, Kowalsky AH, Cho CS, Semple I, Ro**
612 **SH, Davis C, Brooks SV, Karin M, Wessells RJ, and Lee JH.** Sestrins are evolutionarily conserved
613 mediators of exercise benefits. *Nat Commun* 11: 190, 2020.
- 614 21. **Yang BA, Castor-Macias J, Fraczek P, Cornett A, Brown LA, Kim M, Brooks SV, Lombaert**
615 **IMA, Lee JH, and Aguilar CA.** Sestrins regulate muscle stem cell metabolic homeostasis. *Stem Cell*
616 *Reports* 16: 2078-2088, 2021.
- 617 22. **Rhee SG, and Bae SH.** The antioxidant function of sestrins is mediated by promotion of
618 autophagic degradation of Keap1 and Nrf2 activation and by inhibition of mTORC1. *Free Radic Biol*
619 *Med* 88: 205-211, 2015.
- 620 23. **Hourde C, Vignaud A, Beurdy I, Martelly I, Keller A, and Ferry A.** Sustained peripheral
621 arterial insufficiency durably impairs normal and regenerating skeletal muscle function. *J Physiol Sci*
622 56: 361-367, 2006.
- 623 24. **Mohiuddin M, Lee NH, Moon JY, Han WM, Anderson SE, Choi JJ, Shin E, Nakhai SA, Tran T,**
624 **Aliya B, Kim DY, Gerold A, Hansen LM, Taylor WR, and Jang YC.** Critical Limb Ischemia Induces
625 Remodeling of Skeletal Muscle Motor Unit, Myonuclear-, and Mitochondrial-Domains. *Sci Rep* 9:
626 9551, 2019.
- 627 25. **Paek R, Chang DS, Brevetti LS, Rollins MD, Brady S, Ursell PC, Hunt TK, Sarkar R, and**
628 **Messina LM.** Correlation of a simple direct measurement of muscle pO₂ to a clinical ischemia index
629 and histology in a rat model of chronic severe hindlimb ischemia. *J Vasc Surg* 36: 172-179, 2002.
- 630 26. **Tang GL, Chang DS, Sarkar R, Wang R, and Messina LM.** The effect of gradual or acute
631 arterial occlusion on skeletal muscle blood flow, arteriogenesis, and inflammation in rat hindlimb
632 ischemia. *J Vasc Surg* 41: 312-320, 2005.
- 633 27. **Hsieh PL, Rybalko V, Baker AB, Suggs LJ, and Farrar RP.** Recruitment and therapeutic
634 application of macrophages in skeletal muscles after hind limb ischemia. *J Vasc Surg* 67: 1908-1920
635 e1901, 2018.
- 636 28. **Lee CW, Stabile E, Kinnaird T, Shou M, Devaney JM, Epstein SE, and Burnett MS.** Temporal
637 patterns of gene expression after acute hindlimb ischemia in mice: insights into the genomic
638 program for collateral vessel development. *J Am Coll Cardiol* 43: 474-482, 2004.
- 639 29. **Paoni NF, Peale F, Wang F, Errett-Baroncini C, Steinmetz H, Toy K, Bai W, Williams PM,**
640 **Bunting S, Gerritsen ME, and Powell-Braxton L.** Time course of skeletal muscle repair and gene
641 expression following acute hind limb ischemia in mice. *Physiol Genomics* 11: 263-272, 2002.
- 642 30. **Scalabrin M, Pollock N, Staunton CA, Brooks SV, McArdle A, Jackson MJ, and Vasilaki A.**
643 Redox responses in skeletal muscle following denervation. *Redox Biol* 26: 101294, 2019.
- 644 31. **Espino-Gonzalez E, Tickle PG, Benson AP, Kissane RWP, Askew GN, Egginton S, and Bowen**
645 **TS.** Abnormal skeletal muscle blood flow, contractile mechanics and fibre morphology in a rat model
646 of obese-HFpEF. *J Physiol* 599: 981-1001, 2021.
- 647 32. **Whitehead A, Krause FN, Moran A, MacCannell ADV, Scragg JL, McNally BD, Boateng E,**
648 **Murfitt SA, Virtue S, Wright J, Garnham J, Davies GR, Dodgson J, Schneider JE, Murray AJ, Church**
649 **C, Vidal-Puig A, Witte KK, Griffin JL, and Roberts LD.** Brown and beige adipose tissue regulate
650 systemic metabolism through a metabolite interorgan signaling axis. *Nat Commun* 12: 1905, 2021.

- 651 33. **Motulsky HJ, and Brown RE.** Detecting outliers when fitting data with nonlinear regression -
652 a new method based on robust nonlinear regression and the false discovery rate. *BMC*
653 *Bioinformatics* 7: 123, 2006.
- 654 34. **Meyer G, Czompa A, Reboul C, Csepanyi E, Czegledi A, Bak I, Balla G, Balla J, Tosaki A, and**
655 **Lekli I.** The cellular autophagy markers Beclin-1 and LC3B-II are increased during reperfusion in
656 fibrillated mouse hearts. *Curr Pharm Des* 19: 6912-6918, 2013.
- 657 35. **Goldberg EJ, Schmidt CA, Green TD, Karnekar R, Yamaguchi DJ, Spangenberg EE, and**
658 **McClung JM.** Temporal Association Between Ischemic Muscle Perfusion Recovery and the
659 Restoration of Muscle Contractile Function After Hindlimb Ischemia. *Front Physiol* 10: 804, 2019.
- 660 36. **Hoinoiu B, Jiga LP, Nistor A, Dornean V, Barac S, Miclaus G, Ionac M, and Hoinoiu T.**
661 Chronic Hindlimb Ischemia Assessment; Quantitative Evaluation Using Laser Doppler in a Rodent
662 Model of Surgically Induced Peripheral Arterial Occlusion. *Diagnostics (Basel)* 9: 2019.
- 663 37. **Lemieux P, and Birot O.** Altitude, Exercise, and Skeletal Muscle Angio-Adaptive Responses to
664 Hypoxia: A Complex Story. *Front Physiol* 12: 735557, 2021.
- 665 38. **Sandri M.** Protein breakdown in muscle wasting: role of autophagy-lysosome and ubiquitin-
666 proteasome. *Int J Biochem Cell Biol* 45: 2121-2129, 2013.
- 667 39. **McClung JM, McCord TJ, Keum S, Johnson S, Annex BH, Marchuk DA, and Kontos CD.**
668 Skeletal muscle-specific genetic determinants contribute to the differential strain-dependent effects
669 of hindlimb ischemia in mice. *Am J Pathol* 180: 2156-2169, 2012.
- 670 40. **Aman Y, Schmauck-Medina T, Hansen M, Morimoto RI, Simon AK, Bjedov I, Palikaras K,**
671 **Simonsen A, Johansen T, Tavernarakis N, Rubinsztein DC, Partridge L, Kroemer G, Labbadia J, and**
672 **Fang EF.** Autophagy in healthy aging and disease. *Nature Aging* 1: 634-650, 2021.
- 673 41. **Chun Y, and Kim J.** Autophagy: An Essential Degradation Program for Cellular Homeostasis
674 and Life. *Cells* 7: 2018.
- 675 42. **Gomez-Sanchez R, Yakhine-Diop SM, Rodriguez-Arribas M, Bravo-San Pedro JM, Martinez-**
676 **Chacon G, Uribe-Carretero E, Pinheiro de Castro DC, Pizarro-Estrella E, Fuentes JM, and Gonzalez-**
677 **Polo RA.** mRNA and protein dataset of autophagy markers (LC3 and p62) in several cell lines. *Data*
678 *Brief* 7: 641-647, 2016.
- 679 43. **Komatsu M, Waguri S, Koike M, Sou YS, Ueno T, Hara T, Mizushima N, Iwata J, Ezaki J,**
680 **Murata S, Hamazaki J, Nishito Y, Iemura S, Natsume T, Yanagawa T, Uwayama J, Warabi E, Yoshida**
681 **H, Ishii T, Kobayashi A, Yamamoto M, Yue Z, Uchiyama Y, Kominami E, and Tanaka K.** Homeostatic
682 levels of p62 control cytoplasmic inclusion body formation in autophagy-deficient mice. *Cell* 131:
683 1149-1163, 2007.
- 684 44. **Mishra P, and Chan DC.** Metabolic regulation of mitochondrial dynamics. *J Cell Biol* 212: 379-
685 387, 2016.
- 686 45. **Dunlop EA, and Tee AR.** mTOR and autophagy: a dynamic relationship governed by nutrients
687 and energy. *Semin Cell Dev Biol* 36: 121-129, 2014.
- 688 46. **Rabanal-Ruiz Y, Otten EG, and Korolchuk VI.** mTORC1 as the main gateway to autophagy.
689 *Essays Biochem* 61: 565-584, 2017.
- 690 47. **Li Y, and Chen Y.** AMPK and Autophagy. *Adv Exp Med Biol* 1206: 85-108, 2019.
- 691 48. **Gong L, Wang Z, Wang Z, and Zhang Z.** Sestrin2 as a Potential Target for Regulating
692 Metabolic-Related Diseases. *Front Endocrinol (Lausanne)* 12: 751020, 2021.
- 693 49. **Bajwa A, Wesolowski R, Patel A, Saha P, Ludwinski F, Smith A, Nagel E, and Modarai B.**
694 Assessment of tissue perfusion in the lower limb: current methods and techniques under
695 development. *Circ Cardiovasc Imaging* 7: 836-843, 2014.
- 696 50. **Monteiro Rodrigues L, Silva H, Ferreira H, Renault MA, and Gadeau AP.** Observations on
697 the perfusion recovery of regenerative angiogenesis in an ischemic limb model under hyperoxia.
698 *Physiol Rep* 6: e13736, 2018.
- 699 51. **Kim J, Lim YM, and Lee MS.** The Role of Autophagy in Systemic Metabolism and Human-
700 Type Diabetes. *Mol Cells* 41: 11-17, 2018.

- 701 52. **Lin XL, Xiao WJ, Xiao LL, and Liu MH.** Molecular mechanisms of autophagy in cardiac
702 ischemia/reperfusion injury (Review). *Mol Med Rep* 18: 675-683, 2018.
- 703 53. **Folker ES, and Baylies MK.** Nuclear positioning in muscle development and disease. *Front*
704 *Physiol* 4: 363, 2013.
- 705 54. **Roman W, and Gomes ER.** Nuclear positioning in skeletal muscle. *Semin Cell Dev Biol* 82: 51-
706 56, 2018.
- 707 55. **Pipinos II, Swanson SA, Zhu Z, Nella AA, Weiss DJ, Gutti TL, McComb RD, Baxter BT, Lynch**
708 **TG, and Casale GP.** Chronically ischemic mouse skeletal muscle exhibits myopathy in association
709 with mitochondrial dysfunction and oxidative damage. *Am J Physiol Regul Integr Comp Physiol* 295:
710 R290-296, 2008.

711

Skeletal muscle remodelling post hindlimb ischemia



A complex interplay between Sestrins-AMPK to regulate autophagy signalling in early-to-late hindlimb ischemia appears to be central for muscle remodelling.

Figure 1

a

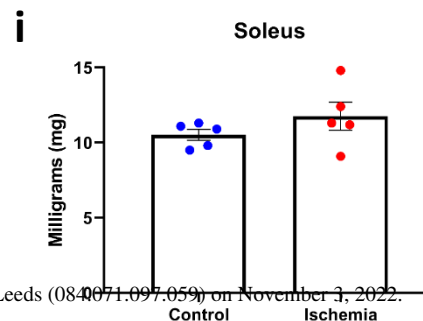
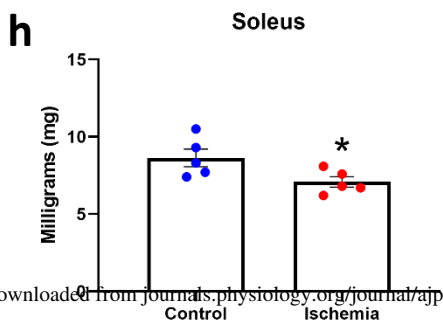
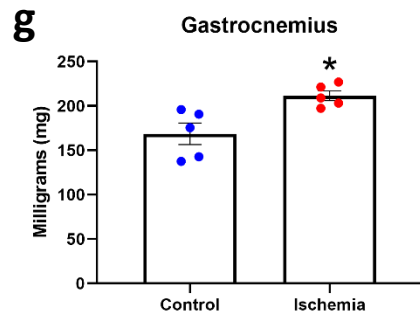
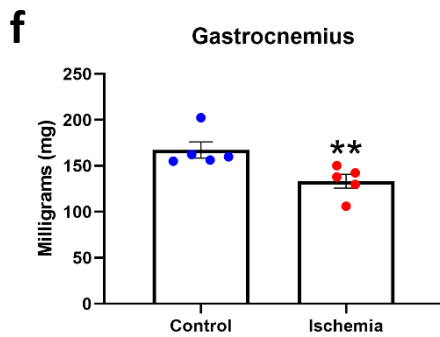
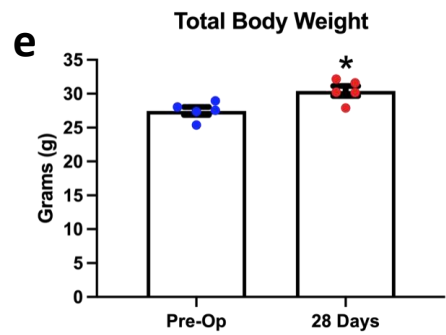
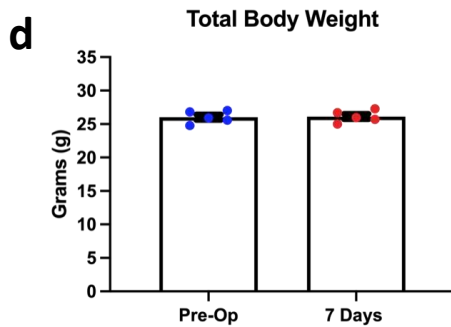
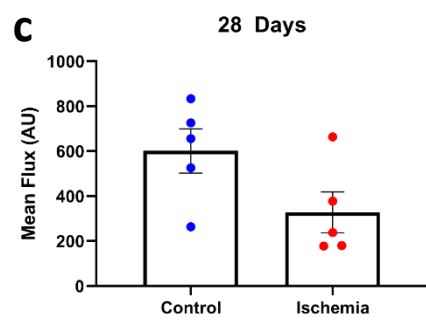
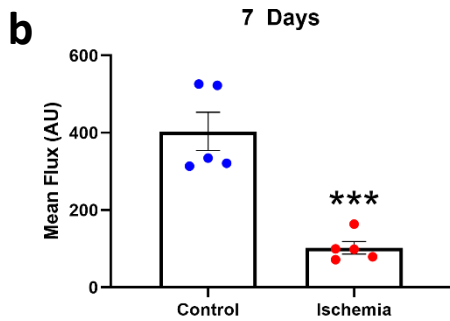
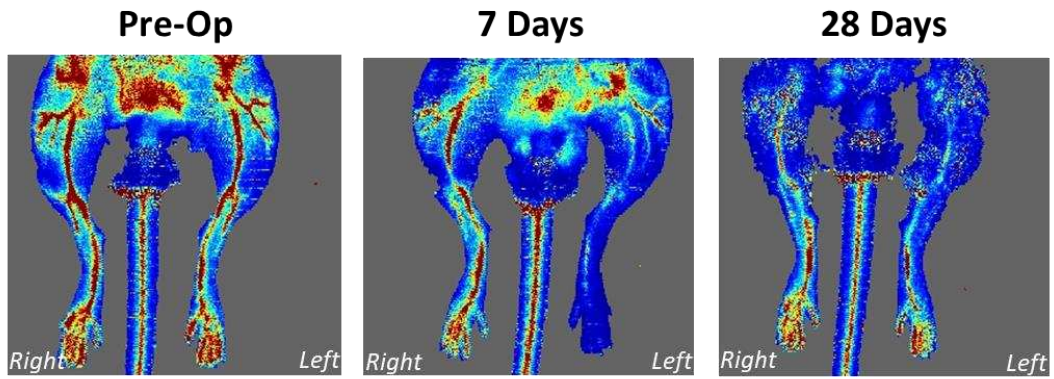
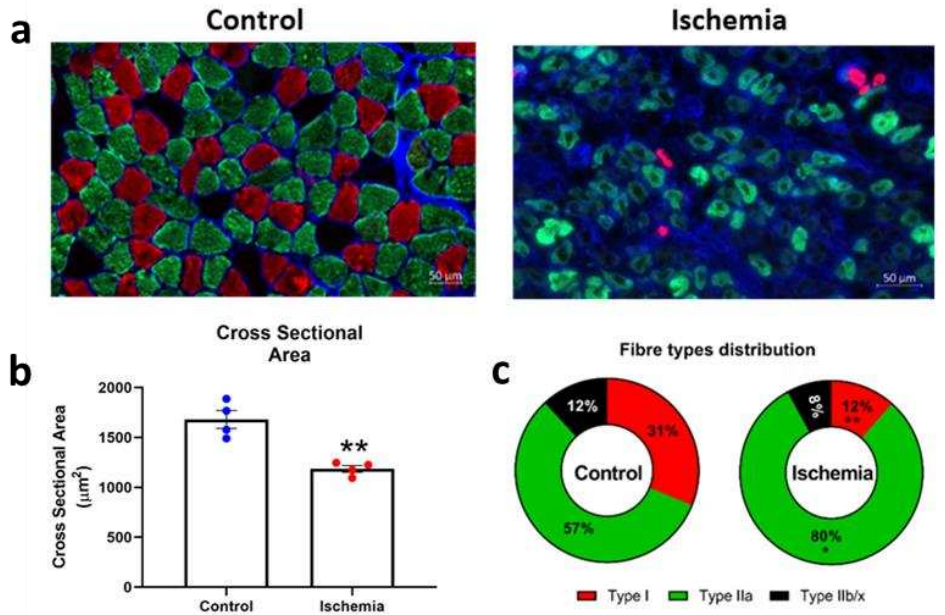
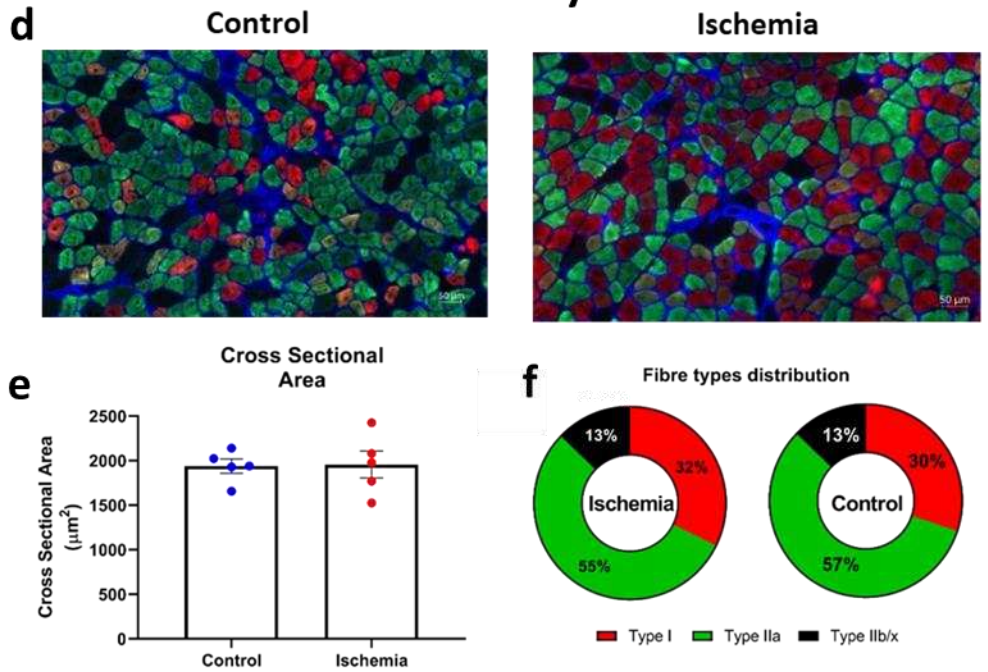


Figure 2

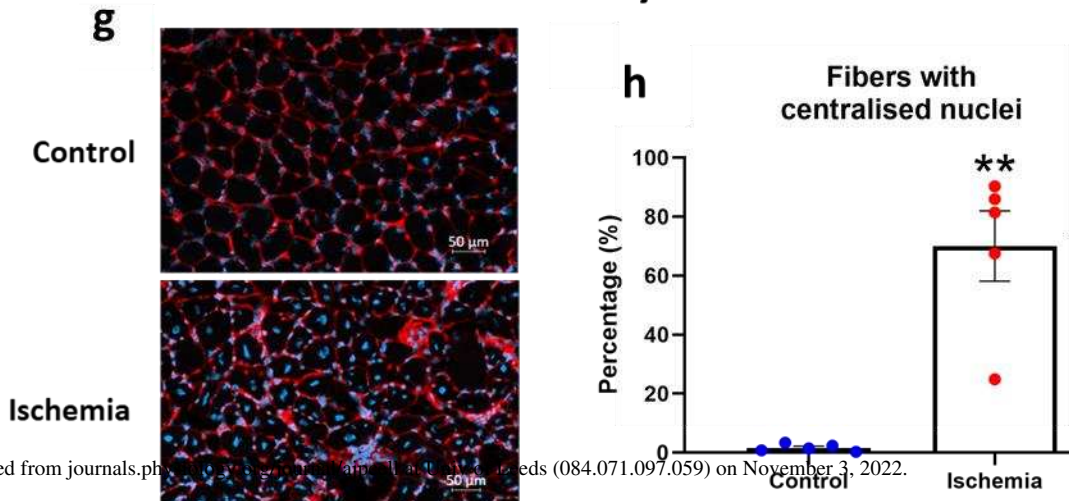
7 Days



28 Days



28 Days



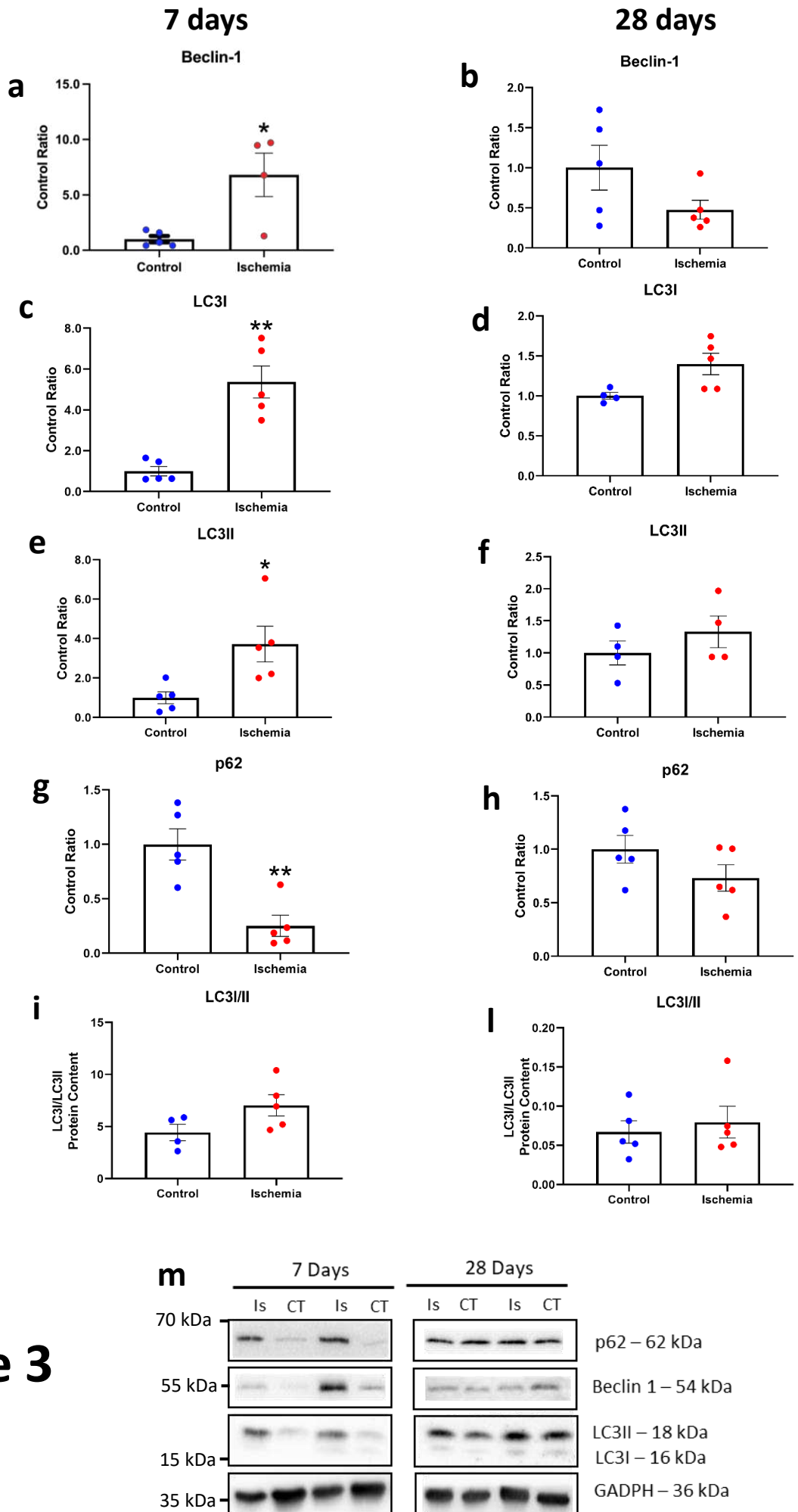


Figure 3

Figure 4

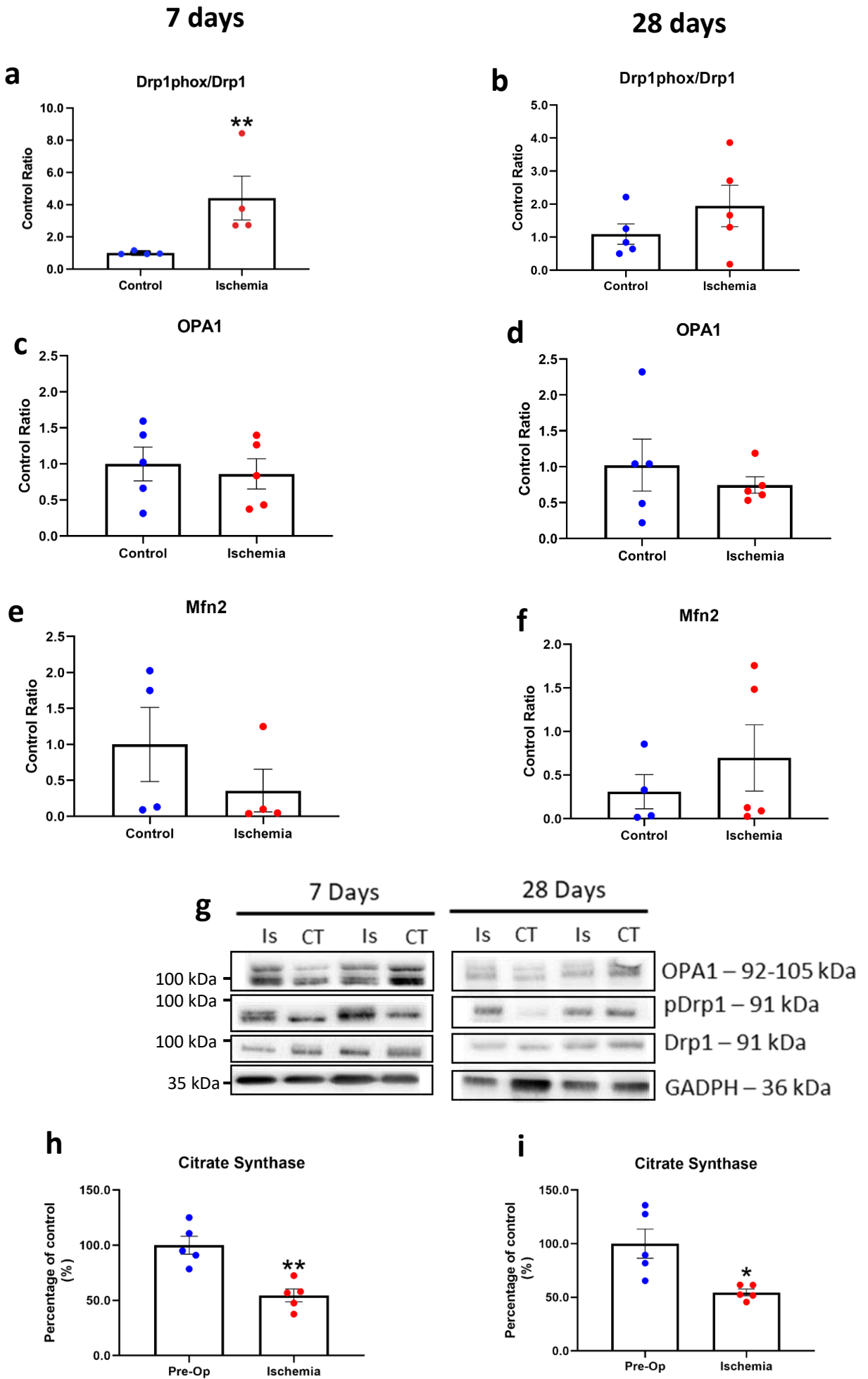


Figure 6

7 Days

28 Days

